



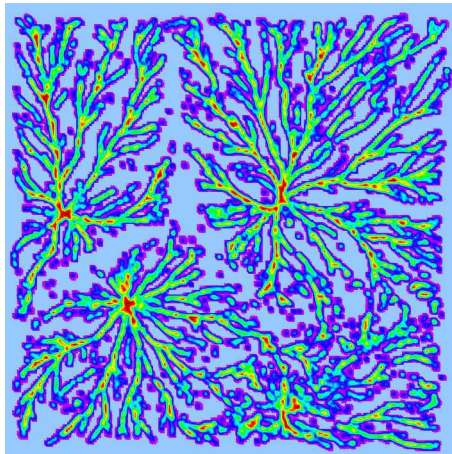
OXFORD CENTRE FOR COLLABORATIVE APPLIED MATHEMATICS

Report Number 09/12

**From Individual to Collective Behavior of  
Unicellular Organisms: Recent Results and  
Open Problems**

by

**Chuan Xue, Hans G. Othmer, Radek Erban**



Oxford Centre for Collaborative Applied Mathematics  
Mathematical Institute  
24 - 29 St Giles'  
Oxford  
OX1 3LB  
England



# From Individual to Collective Behavior of Unicellular Organisms: Recent Results and Open Problems

Chuan Xue\*

Hans G. Othmer<sup>†</sup>

Radek Erban<sup>‡</sup>

March 2, 2009

**Abstract.** The collective movements of unicellular organisms such as bacteria or amoeboid (crawling) cells are often modeled by partial differential equations (PDEs) that describe the time evolution of cell density. In particular, chemotaxis equations have been used to model the movement towards various kinds of extracellular cues. Well-developed analytical and numerical methods for analyzing the time-dependent and time-independent properties of solutions make this approach attractive. However, these models are often based on phenomenological descriptions of cell fluxes with no direct correspondence to individual cell processes such as signal transduction and cell movement. This leads to the question of how to justify these macroscopic PDEs from microscopic descriptions of cells, and how to relate the macroscopic quantities in these PDEs to individual-level parameters. Here we summarize recent progress on this question in the context of bacterial and amoeboid chemotaxis, and formulate several open problems.

## 1 Introduction

In view of the enormous complexity of many biological problems, it is reasonable to assert that ‘biology will inspire and motivate new mathematics in the years to come, much as physics has done for many centuries’<sup>1</sup>. We follow the spirit of this philosophy in this contribution, and summarize recent progress in embedding certain aspects of cell-level biology into population-level equations in the context of taxis-driven movement of unicellular organisms. We also formulate several open mathematical problems.

We begin with a simple random walk model and its connection to a partial differential equation in Section 2.1. This classical example will illustrate basic relations between random walks and PDEs. In Section 2.2 and 2.3, we present examples of more complicated random walks that are abstracted from the biology of unicellular organisms, and summarize recent results on mapping the microscopic stochastic processes that describe cell movement to macroscopic equations for cell density. In Section 3, we define two classes of random walks that include the biological models from Section 2. We will call them random walks with internal dynamics of type P (when spatial variations in intracellular variables are ignored and cells are treated as points) and type D (when the internal state variables of interest vary within the cell). The former applies to small cells such as bacteria, while the latter applies to larger amoeboid cells. Both types lead to a number of open mathematical problems, and a mathematician who is less interested in the biological motivation can find these problems in Section 3. On the other hand, a biologist who is more interested in how this area of mathematical biology relates to his/her research can focus on Section 2.

---

\*Mathematical Biosciences Institute, Ohio State University, Columbus, OH 43210, USA; e-mail: cxue@mbi.osu.edu

<sup>†</sup>School of Mathematics, University of Minnesota, Minneapolis, MN 55455, USA, email: othmer@math.umn.edu

<sup>‡</sup>Mathematical Institute, University of Oxford, 24-29 St Giles’, Oxford, OX1 3LB, UK, e-mail: erban@maths.ox.ac.uk

<sup>1</sup>This is a contribution to the proceedings of 2<sup>nd</sup> Okinawa Conference on Mathematics and Biology. The quote is borrowed from the website of conference organizers, which, at the time of the publication, appears at [http://www.oist.jp/faculty\\_sinclair.html](http://www.oist.jp/faculty_sinclair.html).

## 2 From individual to collective behavior of unicellular organisms

Motile organisms can sense their environment and respond to it (i) by directed movement toward or away from a signal, which is called *taxis*, (ii) by changing their speed and/or turning frequency, which is called *kinesis*, or (iii) by a combination of these. The first is chemotaxis and the second chemokinesis if the signal is a chemical, but despite their differences, the two are collectively referred to as chemotaxis. Chemotaxis involves: (i) the extracellular signal, (ii) the signal transduction machinery that transduces the extracellular signal into an intracellular signal, and (iii) changes in the motile behavior of the cells in response to the intracellular signal. To move away from repellents or toward attractants organisms must extract directional information from the extracellular signal, which is usually a scalar field, and there are two distinct strategies that are used to do this.

The first strategy is used by bacterial cells, which detect the signal intensity at the present location, move away, measure the signal again and from a comparison of the two decide on the next step. Thus they measure the temporal variation in the signal as they move through the external field (*cf.* [9] and references therein). Cells that are large enough to detect typical differences in the signal over their body length, e.g., amoeboid cells, employ the second strategy: these cells make a ‘two-point-in-space’ measurement, compare the signals, and crawl towards better conditions. In either case, another consideration in understanding population-level behavior is whether or not an individual merely detects the signal and responds to it, or whether the individual alters it as well, for example by consuming it or by amplifying it so as to relay the signal. In the former case there is no feedback from the local density of individuals to the external field, but when the individual produces or degrades the signal, there is coupling between the local density of individuals and the intensity of the signal. The latter occurs during aggregation of the slime mold *Dictyostelium discoideum*, where cells move up the gradient of cAMP and relay cAMP as well [27, 36], and in pattern formation by the bacterium *E. coli* discussed later in Section 2.2.

Although the details of the two strategies used by cells during chemotaxis are very different, the same classical Patlak-Keller-Segel (PKS) chemotaxis equations

$$\frac{\partial n}{\partial t} = \nabla \cdot (D_n \nabla n - \chi n \nabla S), \quad (1)$$

$$\frac{\partial S}{\partial t} = D_s \Delta S + f(n, S). \quad (2)$$

and its variant forms have been widely used to model the population density in response to external signals. Here  $n$  is the cell density,  $S$  is the signal concentration,  $D_n$  and  $D_s$  are the diffusion constants, and  $\chi$  is the chemotaxis sensitivity. Questions of existence and uniqueness of solutions, pattern formation, and in particular aggregation, and the dependence of these properties on the nature and strength of the chemotactic response have been widely studied [16]. However, the general problem of justifying the macroscopic equations from the microscopic details of signal transduction and movement, and translating the microscopic parameters into macroscopic quantities in different contexts remains a challenge. Some progress on this has been made recently in the background of both swimming bacteria and crawling eukaryotic cells [15, 26, 8, 9, 10, 38]. In the following we begin with a simple example in Section 2.1, and summarize the main results for bacteria in Section 2.2 and for crawling cells in Section 2.3.

### 2.1 The telegraph process in the absence of internal dynamics

How the PKS equation (1) relates to the movement of individuals can be understood in the context of a stochastic process called the telegraph process. In this process, which we call the telegraph random walk (TRW), a particle whose position is  $x \in \mathbb{R}$  moves with speed  $s$  in either direction. The particle changes its direction according to a Poisson process with constant turning frequency  $\lambda_0 > 0$ . It can be simulated as follows: choose a small time step  $\Delta t$  and update the position of a particle as  $x(t + \Delta t) = x(t) \pm s \Delta t$  where  $\pm s$  is its velocity at time  $t$ . At each time step, generate a random number  $r$  uniformly distributed in  $(0, 1)$ , and if  $r < \lambda_0 \Delta t$  the particle changes direction, and otherwise it continues. Three realizations of

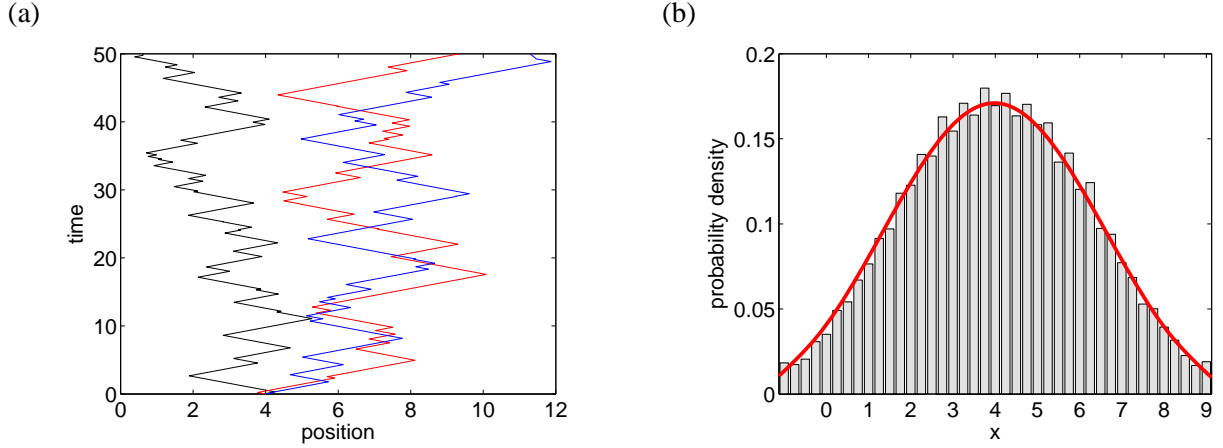


Figure 1: (a) *Three random trajectories generated by the TRW for  $\lambda_0 = s = 1$ .* (b) *The histogram of particle distribution obtained by a simulation of 10,000 particles (gray) and by solution of the macroscopic equation (3) (red line).*

trajectories of particles for the TRW are shown in Figure 1(a). Since the TRW process is stochastic, different realizations that begin at the same initial point are different, but the average behavior of many particles, each executing the TRW, is deterministic.

In biological applications the quantity of interest is often this average, which is represented by the density  $n(x, t)$  of particles at point  $x$  and time  $t$ . This satisfies the macroscopic telegrapher's equation [14, 18]

$$\frac{\partial^2 n}{\partial t^2} + 2\lambda_0 \frac{\partial n}{\partial t} = s^2 \frac{\partial^2 n}{\partial x^2}. \quad (3)$$

In Figure 1(b), we show the density profile predicted from (3) (red line), compared with a histogram of positions of 10,000 particles that started at  $x(0) = 4$  and follow the TRW. One sees that stochastic fluctuations around the mean are relatively small, and the density profile does not change significantly for other realizations using 10,000 particles.

Equation (3) shares some similarities with (1)-(2), but the fundamental difference between them is that the coefficients of (3) are written in terms of the parameters  $\lambda_0$  and  $s$  of the TRW. That is, the parameters of the individual-level behavior fully determine the macroscopic evolution of the density given by (3). The PKS system also contains coefficients that should reflect cell-level behavior, but until recently there was no mechanism for relating micro- and macroscopic parameters. We will address this problem in Section 2.2 and 2.3.

The macroscopic equation (3) has been derived rigorously in [18], and the associated TRW has been studied by many authors [14, 18, 28]. The exact solution of (3) can be obtained by a variety of methods and it can be shown from the exact solution that the TRW is approximated by a diffusion process in a suitable limit. The motivation for finding macroscopic equations rests in the facts that (a) there are many established techniques for the analysis of PDEs that lead to a qualitative understanding of how various processes interact to affect the solutions, and (b) we can bypass the computationally-intensive individual-based simulations by solving the macroscopic PDEs. Progress toward the micro-to-macro transition for the PKS system is reported in [34, 24]. In the remainder of the paper we present more complicated examples of random walks that are used for modeling the behavior of unicellular organisms, we summarize recent results on the derivation of macroscopic PDEs starting from the evolution equation for a phase-space density, and we formulate open problems in this field.

## 2.2 Individual-level behavior of flagellated bacteria and macroscopic PDEs

Many flagellated bacteria such as *E. coli* swim using a run-and-tumble strategy in which movement consists of more-or-less straight runs interrupted by tumbles [2, 4]. When rotated counterclockwise the flagella form a bundle that propels the cell forward with a speed  $s \sim 10 - 30 \mu\text{m/s}$ ; when rotated clockwise the bundle flies apart and the cell ‘tumbles’. Tumbles reorient the cells in a more-or-less randomly-chosen direction, with a slight bias in the direction of the previous run, for the next run [3]. The run and tumble movement is a 3D analog of the TRW, and in the absence of signal gradients the random walk is unbiased, with a mean run time  $\sim 1$  s and a tumble time  $\sim 0.1$ s. However, when exposed to an external signal gradient, the cell responds by increasing (decreasing) the run length when moving towards (away from) a favorable direction, and therefore the random walk is biased with a drift in that direction [1, 19]. The coordinated movement of these bacteria can lead to a variety of cell density patterns including networks, localized aggregation and traveling waves (Figure 2).

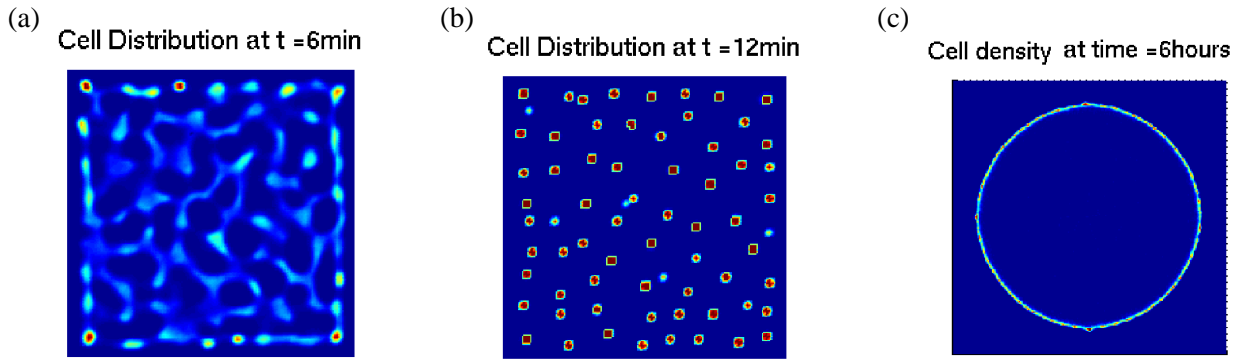


Figure 2: *Simulated E. coli patterns by a cell-based model. (a) Network formation from an uniform cell lawn; (b) Aggregate formation from the network; (c) Traveling wave formation from a single inoculum in the center. Adapted from [29] with permission.*

The TRW is an example of a larger class of random walks called velocity-jump processes [25]. Bacteria such as *E. coli* are typically small ( $\sim 1\mu\text{m}$  in length), and for movement purposes can be characterized as point particles with position  $\mathbf{x} \in \mathbb{R}^N$  and velocity  $\mathbf{v} \in V \in \mathbb{R}^N$ . By approximating the relatively short tumbling stage as an instantaneous jump, individual movement is described as a velocity jump process [25], and the statistics of movement of cells can be described by the probability density  $p$ , which evolves according to the transport equation

$$\frac{\partial}{\partial t} p(\mathbf{x}, \mathbf{v}, t) + \mathbf{v} \cdot \nabla p(\mathbf{x}, \mathbf{v}, t) = -\lambda p(\mathbf{x}, \mathbf{v}, t) + \lambda \int_V T(\mathbf{v}, \mathbf{v}') p(\mathbf{x}, \mathbf{v}', t) d\mathbf{v}'. \quad (4)$$

Here  $\lambda$  is the turning rate and  $T(\mathbf{v}', \mathbf{v})$  is the turning kernel. When the cells are well separated and there is little mechanical interaction between them,  $p$  can also be regarded as the cell density as a function of  $\mathbf{x}$ ,  $\mathbf{v}$  and  $t$ . The observed macroscopic density  $n$  is an integral of  $p$  over all variables other than space and time, *i.e.*,  $n = \int_V p d\mathbf{v}$  here.

In the absence of a signal gradient  $\lambda$  is a constant ( $= \lambda_0$ ), and on suitable time and space scales, and under suitable hypotheses on the turning kernel  $T$ , this velocity-jump process reduces to a diffusion process [15]. In the diffusion equation

$$\frac{\partial n}{\partial t} = \nabla \cdot (D_n \nabla n) \quad (5)$$

that results, the macroscopic coefficient  $D_n$  can in general be a second-rank tensor, but when  $T$  is symmetric it is a scalar and  $D_n = s^2 / (N(1 - \psi_d)\lambda_0)$  where  $N$  is the spatial dimension and  $\psi_d$  is the so-called index of directional persistence that characterizes  $T$  [15]. In the presence of a chemical signal the PKS chemotaxis equation (1) was derived in the diffusion limit by assuming that the extracellular signal field  $S$  enters via

small perturbations of the unstimulated turning rate  $\lambda$  [26]. The essential assumption was that the time scale for the microscopic random walk is well separated from the transport and diffusion time scales.

Experimental advances have led to extensive study of the mechanisms of bacterial chemotaxis, and much is known for the model system *E. coli*. Therefore representations of the macroscopic chemotactic sensitivity in terms of parameters that characterize the microscopic intracellular signal transduction network became possible, which was carried out in a sequence of papers [8, 9, 38]. In [8] internal state variables were introduced to describe the time-dependent signal transduction and response. When this is done the transport equation becomes

$$\frac{\partial p}{\partial t} + \nabla_x \cdot (\mathbf{v}p) + \nabla_y \cdot (\mathbf{f}p) = -\lambda(\mathbf{y})p + \int_V \lambda(\mathbf{y})T(\mathbf{v}, \mathbf{v}', \mathbf{y})p(\mathbf{x}, \mathbf{v}', \mathbf{y}, t) d\mathbf{v}', \quad (6)$$

where

$$\frac{d\mathbf{y}}{dt} = \mathbf{f}(\mathbf{y}, S(\mathbf{x}, t)) \quad (7)$$

models signal transduction and  $\lambda(\mathbf{y})$  describes the motor response. The entire signal transduction of bacteria is very complicated and detailed models involve many state variables [33], but the major processes consist of fast excitation in response to signal changes and slow adaptation that subtracts out the background signal. These processes can be captured by the cartoon description

$$\frac{dy_1}{dt} = \frac{G(S(\mathbf{x}, t)) - (y_1 + y_2)}{t_e}, \quad (8)$$

$$\frac{dy_2}{dt} = \frac{G(S(\mathbf{x}, t)) - y_2}{t_a}. \quad (9)$$

Here  $G(S)$  models signal detection via surface receptors and  $t_e$  and  $t_a$  specify the excitation and adaptation time scales, with  $t_e \ll t_a$ . Using this cartoon description for  $\mathbf{f}$ , applying moment closure techniques and a regular perturbation method, the macroscopic equation

$$\frac{\partial n}{\partial t} = \nabla \cdot \left[ \frac{s^2}{N\lambda_0} \nabla n - G'(S(x, t)) \frac{bs^2 t_a}{N\lambda_0(1 + \lambda_0 t_a)(1 + \lambda_0 t_e)} n \nabla S \right], \quad (10)$$

with  $b = -\frac{\partial \lambda}{\partial y_1}|_{y_1=0}$  was first derived in 1D in [8], and later extended to 3D in [9]. The major assumption in this derivation is that the signal gradient is shallow, *i.e.*,  $G'(S)\nabla S \cdot \mathbf{v} \sim \mathcal{O}(\varepsilon) \text{ sec}^{-1}$ , and  $t_a \lambda_0 \sim \mathcal{O}(1)$ , which results in a clear separation of the microscopic time scales from the macroscopic transport and diffusion time scales. Other assumptions include time-independent signals  $S = S(\mathbf{x})$ , a linear turning rate  $\lambda = \lambda_0 - by_1$  and no directional persistence  $\psi_d = 0$ . New moment closure methods were developed in [38] to generalize the derivation for time dependent signals  $S = S(\mathbf{x}, t)$  and nonlinear dependence of the turning rate on internal variables  $\lambda = \lambda_0 - by_1 + a_2 y_1^2 - \dots$  with the previous case corresponds to  $a_i = 0$ , for all  $i \geq 2$ . The shallow gradient assumption becomes  $\frac{b}{\lambda_0} G'(S)(\nabla S \cdot \mathbf{v} + \frac{\partial S}{\partial t}) \sim \mathcal{O}(\varepsilon) \text{ sec}^{-1}$  and the same equation (10) was derived under this condition with directional persistence appearing as a scaling of the turning rates by a factor of  $(1 - \psi_d)$ . The method also works for any finite system of internal dynamics  $f(\mathbf{y})$  in polynomial form under the assumption of separability of microscopic and macroscopic time scales.

Cell movement in the presence of multiple signals and external forces was also considered in [38]. Many cells have multiple receptor types and thus can respond to many different signals. How a cell integrates these different signals and responds properly is not known in general, but in bacteria different signaling pathways share the same network downstream of the receptors, and therefore different signals are integrated at the signal processing step. In this case, the function  $G$  is generally a function of all signals,  $G = G(S_1, S_2, \dots, S_m)$ , and the macroscopic equation for cell density becomes

$$\frac{\partial n}{\partial t} = \nabla \cdot \left[ D_n \nabla n - \chi_0 n \left( \frac{\partial G}{\partial S_1} \nabla S_1 + \dots + \frac{\partial G}{\partial S_m} \nabla S_m \right) \right], \quad (11)$$

where

$$D_n = \frac{s^2}{N\lambda_0(1-\psi_d)} \quad \text{and} \quad \chi_0 = \frac{bs^2t_a}{N\lambda_0(1+\lambda_0(1-\psi_d)t_a)(1+\lambda_0(1-\psi_d)t_e)}.$$

Other generalizations are possible. For example, bacteria generally swim in more complicated environments with external forces acting on them, and macroscopic equations can be derived from a velocity jump process with acceleration terms. As an example, when cells swim close to a surface, the runs are curved to the right when observed from above [7] due to an imbalance of viscous force on the cell body, and this bias has been shown to induce spiral density patterns [37]. By treating the swimming bias as an external force, the macroscopic equation

$$\frac{\partial n}{\partial t} = D_n \Delta n - \nabla \cdot \left[ G'(S)n \left( \chi_0 \nabla S + \beta_0 (\nabla S)^\perp \right) \right] \quad (12)$$

has been derived in two space dimensions in [38]. Here  $(\nabla S)^\perp = ((\nabla S)_2, (-\nabla S)_1)^T$  is a vector orthogonal to  $\nabla S$ , and the diffusion coefficient and the chemotactic sensitivities under the assumption of fast excitation are as follows:

$$\begin{aligned} D_n &= \frac{s^2}{2\lambda_0(1-\psi_d) + \frac{2\omega_0^2}{\lambda_0(1-\psi_d)}}, \\ \chi_0 &= \frac{b(1-\psi_d)s^2[\lambda_0(1-\psi_d)(\lambda_0(1-\psi_d) + \frac{1}{t_a}) - \omega_0^2]}{2((\lambda_0(1-\psi_d) + \frac{1}{t_a})^2 + \omega_0^2)(\lambda_0^2(1-\psi_d)^2 + \omega_0^2)}, \\ \beta_0 &= \frac{\omega_0 b(1-\psi_d)s^2(2\lambda_0(1-\psi_d) + \frac{1}{t_a})}{2((\lambda_0(1-\psi_d) + \frac{1}{t_a})^2 + \omega_0^2)(\lambda_0^2(1-\psi_d)^2 + \omega_0^2)}. \end{aligned} \quad (13)$$

The parameter  $\omega_0$  measures the swimming bias, while  $\psi_d$  is the index of directional persistence. Notice that the swimming bias decreases the diffusion coefficient and the chemotactic sensitivity  $\chi_0$ , and introduce a drift or a second taxis-like term in the direction orthogonal to the signal gradient. Also notice that  $\psi_d$  appears only in the scaling factor of the turning rate constants  $\lambda_0$  and  $b$ . The method developed in [38] can be used to incorporate the effect of more general imposed forces as well.

### 2.3 The route from individual-level descriptions of amoeboid cells to macroscopic PDEs

The directed motion of eukaryotic cells (for example, *Dictyostelium discoideum* (Dd) or leukocytes) is more complicated than bacterial motion. Cells detect extracellular chemical and mechanical signals via membrane receptors, and these trigger signal transduction cascades that produce intracellular signals. Small differences in the extracellular signal over the cell are amplified into large end-to-end intracellular differences that control the motile machinery of the cell and thereby determine the spatial localization of contact sites with the substrate and the sites of force-generation needed to produce directed motion [32, 5]. For instance, well-polarized Dd cells are able to detect and respond to chemoattractant gradients with as little as a 2% concentration difference between the anterior and posterior of the cell [23]. Directional changes of a shallow gradient induce polarized cells to turn on a time scale of 2-3 seconds [13], whereas large changes lead to large-scale disassembly of motile components and creation of a new “leading edge” directed toward the stimulus [12].

Thus the first important difference from the bacterial case is that any individual-based model of Dd that purports to provide at least a caricature description of direction sensing and movement cannot treat cells as points, but must allow for spatial variations in the finite cell volume (or area in 2D). There are a number of models for how cells extract directional information from the cAMP field. An early suggestion was that directional information is obtained by the extension of pseudopods bearing cAMP receptors, and that sensing the temporal change experienced by a receptor is equivalent to sensing the spatial gradient [11]. However,

more recent experiments show that cells in a steady gradient can polarize in the direction of the gradient without extending pseudopods [32]. Thus cells must rely entirely on differences in the signal across the cell body for orientation. Moreover, the timing between different components of the response is critical, because a cell must decide how to move before it begins to relay the signal. Analysis of a model for the cAMP relay pathway, in which cells are treated as squat cylinders, shows that a cell experiences a significant difference in the front-to-back ratio of cAMP when a neighboring cell begins to signal [6], which demonstrates that sufficient end-to-end differences for reliable orientation can be generated for typical extracellular signals; all that is needed is that the direction-sensing pathways respond at least as fast as the cAMP pathway. More recently, a number of simplified models of directional sensing in eukaryotic chemotaxis have been developed [17, 22, 21]. The model used in [6] produces realistic aggregation when suitable formal rules for cell movement are used, as shown in Figure 3.

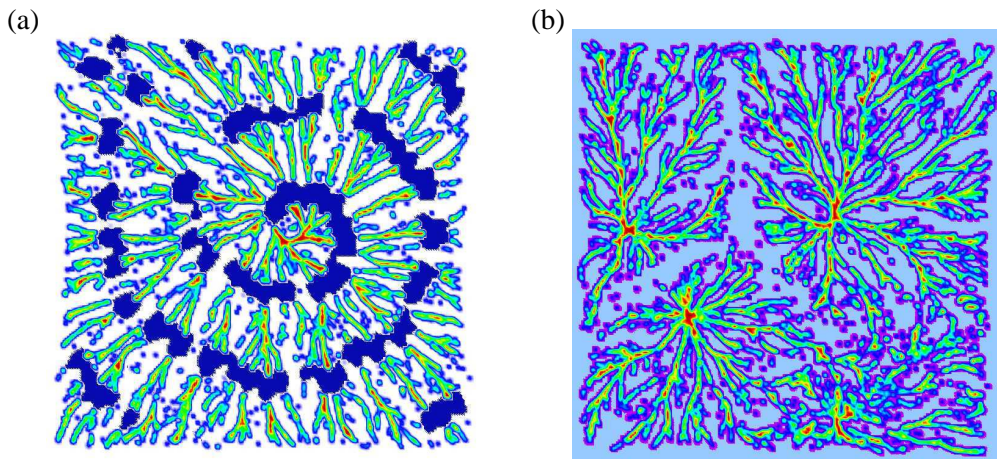


Figure 3: Aggregation patterns in *Dd* predicted by a cell-based model with realistic cAMP intracellular dynamics and formal movement rules. (a): a single aggregation center showing cell streams and a superimposed spiral cAMP wave (blue), and (b) several competing aggregation centers. From [6] with permission.

The second complication that must be dealt with is that the force-generation machinery that drives the motion of eukaryotic cells plays a central role in the macroscopic response of these cells to chemotactic signals. In the ‘run-and-tumble’ description of bacterial motion we assumed that jumps were instantaneous (*i.e.*, forces were Dirac distributions) and the bacterial behavior was described as a velocity jump process. Moreover, the reduction to a diffusion process can still be carried through if there is a finite lifetime in the tumble state, as long as the transitions are instantaneous [26]. In contrast, the directional changes in eukaryotic cells are much slower and depend directly on the signal location, and thus this has to be included in the model. This has been done at the single cell level, using a model for intracellular cAMP dynamics, and treating the cells as deformable viscoelastic ellipsoids that exert forces on the substrate and one another. This more complex model also produces realistic aggregation patterns, as shown in Figure 4, but there is a huge gap between realistic, single-cell models and continuum descriptions. Thus far only relatively simple cell-based models have been used for the derivation of macroscopic descriptions, for the reasons elaborated below.

Following [6, 10, 21], a cell is described as  $B_\varrho = \{\xi \in \mathbb{R}^N \mid \|\xi\| \leq \varrho\}$  where  $N = 2$  or  $N = 3$  is the dimension of the physical space, *i.e.*,  $B_\varrho$  is a circle (for  $N = 2$ ) or a sphere (for  $N = 3$ ). The model of an eukaryotic cell is formulated in terms of the position of its center  $\mathbf{x} \in \mathbb{R}^N$ , its velocity  $\mathbf{v} \in \mathbb{R}^N$ , its internal state functions  $\mathbf{y} : B_\varrho \rightarrow \mathbb{R}^{d_1}$  and its membrane state functions  $\mathbf{z} : \partial B_\varrho \rightarrow \mathbb{R}^{d_2}$ . We denote by  $\bar{\mathbf{y}} = (\mathbf{y}, \mathbf{z}) \in \mathbb{Y}$  the combined internal and membrane state. Here  $\mathbb{Y}$  is a suitable, in general infinite-dimensional, Banach space.

The force per unit mass on the centroid of a cell is denoted by  $\mathcal{F}(\mathbf{x}, \mathbf{v}, \bar{\mathbf{y}})$ , and the internal state and

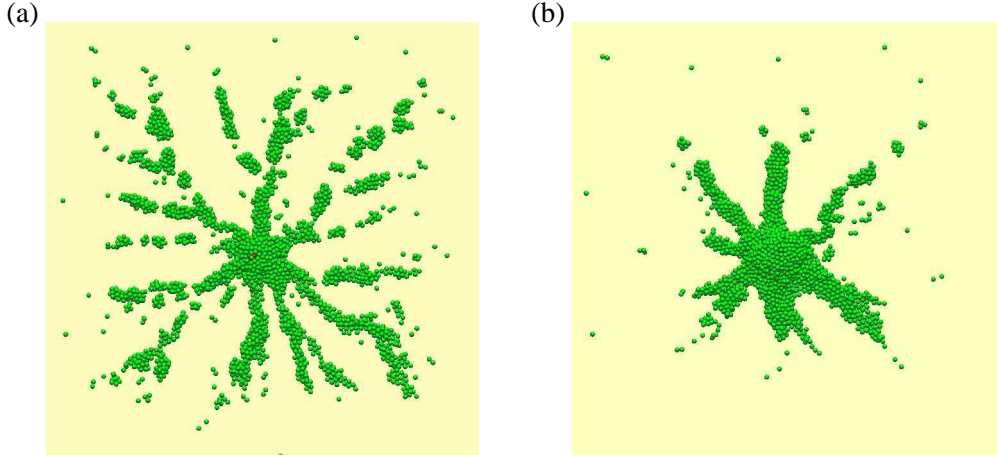


Figure 4: *Intermediate (a) and late-stage (b) aggregation patterns in  $Dd$  predicted by a cell-based model with cAMP dynamics, directional sensing and orientation, and cell-cell and cell-substrate interactions. From [31] with permission.*

velocity are assumed to evolve according to

$$\frac{d\bar{\mathbf{y}}}{dt} = \mathcal{G}(\bar{\mathbf{y}}, S), \quad (14)$$

$$\frac{d\mathbf{v}}{dt} = \mathcal{F}(\mathbf{x}, \mathbf{v}, \bar{\mathbf{y}}), \quad (15)$$

where  $\mathcal{G} : \mathbb{Y} \times \mathbb{S} \rightarrow \mathbb{Y}$  is a mapping between Banach spaces and  $\mathcal{F} : \mathbb{R}^N \times \mathbb{R}^N \times \mathbb{Y} \rightarrow \mathbb{R}^N$ . This generality is needed because the combined internal state  $\bar{\mathbf{y}}$  includes quantities that depend on the location in the cell or on the membrane, and which may, for example, satisfy a reaction-diffusion equation or another evolution equation. The example of (14) that will be used in Section 3 (Random walk D) is the reaction-diffusion equation for  $\mathbf{y}$

$$\frac{\partial \mathbf{y}}{\partial t} = D\Delta \mathbf{y} + \mathbf{f}(\mathbf{y}), \quad \text{in } B_\varrho, \quad (16)$$

$$b(\mathbf{y}, \mathbf{z}) = 0, \quad \text{in } \partial B_\varrho. \quad (17)$$

Thus the boundary condition for  $\mathbf{y}$  involves a relation between it and the membrane state functions  $\mathbf{z}$ , perhaps to reflect binding or other processes such as scaffold formation. The boundary variables in turn evolve according to the equation

$$\frac{\partial \mathbf{z}}{\partial t} = \mathbf{g}(\mathbf{z}, S), \quad \text{in } \partial B_\varrho, \quad (18)$$

where  $S$  is the external signal, and this could also incorporate diffusion on the boundary by suitably altering the equation. The equation (15) is in general a stochastic differential equation that can incorporate the random processes observed in cells, and thus the individual-based behavior is formulated as a random walk.

The derivation of macroscopic equations for eukaryotic cells is a challenging task. A simple model of the form (14-15) for a single cell is studied in [10]. This model captures the essential features of cell movement in response to traveling waves of chemoattractant. Moreover, there exists a mapping  $\mathcal{P} : \mathbb{Y} \rightarrow \mathbb{R}^k$ ,  $k < \infty$ , satisfying  $\mathcal{F}(\mathbf{x}, \mathbf{v}, \bar{\mathbf{y}}) = \mathbf{F}(\mathbf{x}, \mathbf{v}, \mathcal{P}(\bar{\mathbf{y}}))$  where  $\mathbf{F} : \mathbb{R}^N \times \mathbb{R}^N \times \mathbb{R}^k \rightarrow \mathbb{R}^N$  such that a closed evolution equation for the variable  $\bar{\mathbf{z}} = \mathcal{P}(\bar{\mathbf{y}})$  can be derived. Then the cellular random walk written in terms of  $(\mathbf{x}, \mathbf{v}, \bar{\mathbf{y}})$  can be equivalently formulated in terms of the finite-dimensional state variables  $(\mathbf{x}, \mathbf{v}, \bar{\mathbf{z}})$ . In particular, one can formulate an equation for the probability distribution  $p(\mathbf{x}, \mathbf{v}, \bar{\mathbf{z}})$  (compare with the equation (6) written for  $p(\mathbf{x}, \mathbf{v}, \mathbf{y})$  in the bacterial case). Asymptotic analysis of this transport equation leads to a system of macroscopic hyperbolic equations, but it is not known if that system can in turn be reduced to (1); details are given in [10]. The derivation of macroscopic equations for systems when the finite-dimensional reduction  $\mathcal{P} : \mathbb{Y} \rightarrow \mathbb{R}^k$  is not possible is an open problem.

### 3 Open problems

In this section we define several random walks motivated by the foregoing biological examples and formulate several open problems relating to the derivation of macroscopic equations that incorporate microscopic properties of these random walks. Solving these problems will not only lead to new developments in mathematics, but the results will also enhance our understanding of behavior of unicellular organisms. As before, we denote by  $N$  the dimension of the underlying physical space, where  $N = 2$  when cell movements are restricted to a surface and  $N = 3$  when cell moves freely in space. We start with two definitions – a cell of type  $P$  corresponds to bacterial (prokaryotic and smaller) cells and a cell of type  $D$  corresponds to larger cells such as Dd.

**Definition 1** A cell of type  $P$  is a point-like particle described by its position  $\mathbf{x} \in \mathbb{R}^N$ , velocity  $\mathbf{v} \in \mathbb{R}^N$  and internal state  $\mathbf{y} \in \mathbb{R}^d$  where  $d$  is a positive integer.

**Definition 2** A cell of type  $D$  is a ball described by the position of its center  $\mathbf{x} \in \mathbb{R}^N$ , velocity  $\mathbf{v} \in \mathbb{R}^N$ , radius  $\varrho > 0$ , internal state functions  $\mathbf{y} : B_\varrho \rightarrow \mathbb{R}^{d_1}$  and membrane state functions  $\mathbf{z} : \partial B_\varrho \rightarrow \mathbb{R}^{d_2}$ , where  $B_\varrho = \{(x, y, z) \mid \|(x, y, z)\| \leq \varrho\}$ .

**Random walk P:** We consider a cell of type P. Its position evolves according to

$$\frac{d\mathbf{x}}{dt} = \mathbf{v}. \quad (19)$$

The random velocity changes are the results of a Poisson process with turning frequency  $\lambda(\mathbf{y})$ . The probability of a change in velocity from  $\mathbf{v}'$  to  $\mathbf{v}$ , given that a reorientation occurs, is  $T(\mathbf{v}, \mathbf{v}')$ . The internal state evolves according to (7).

**Open Problem 1:** Consider a population of cells of type P that move by Random walk P in a field  $S(\mathbf{x}, t) \in C^\infty(\mathbb{R}^N \times \mathbb{R}^+)$ . The general problem is to derive equations for the cell density from cell-based models with  $\mathbf{f} : \mathbb{R}^{d+1} \rightarrow \mathbb{R}^d$ ;  $\lambda : \mathbb{R}^d \rightarrow (0, \infty)$  and  $T : \mathbb{R}^{2N} \rightarrow (0, \infty)$  under a variety of signal gradients. As shown in Section 2.2, the problem has been investigated for a cartoon description of  $\mathbf{f}$  given by (8)–(9), analytical  $\lambda$  and symmetric  $T$  [9, 8, 38]. Equation (10) has been derived for shallow gradients, *i.e.*,  $H \equiv \frac{b}{\lambda_0} G'(S)(\nabla S \cdot \mathbf{v} + \frac{\partial S}{\partial t}) \sim \mathcal{O}(\varepsilon) \text{ sec}^{-1}$  with  $\varepsilon = s/(L\lambda_0) \approx 10^{-2}$ . The chemotactic sensitivity derived would be zero for  $t_a = 0$ , which agrees with the biological fact that instantaneous adaptation to the signal precludes aggregation. It remains to be determined whether the PKS equation (1) or its variant forms gives a good representation of the population dynamics for bacterial chemotaxis, how the macroscopic quantities relate to microscopic parameters, and if the PKS equation fails under certain cases what macroscopic equation can be derived. In [39] it is shown that for an ultra-small signal gradient,  $H \leq \mathcal{O}(\varepsilon^2) \text{ sec}^{-1}$ , the chemotactic response of the population provides a small perturbation, via higher order terms, of the cell density, which evolves according to a diffusion process with  $D_n = s^2/(N\lambda_0)$ . However, for large signal gradients ( $H \geq \mathcal{O}(1) \text{ sec}^{-1}$ ) equation (10) fails since the macroscopic velocity

$$\mathbf{u}_S = \chi(S)\nabla S = s \left( \frac{bs}{\lambda_0} G'(S)\nabla S \right) \left( -\frac{1}{|V|} \int_V \mathbf{v} \otimes (t_a \lambda_0 \mathcal{A} - 1)^{-1} \mathbf{v} d\mathbf{v} \right) \quad (20)$$

can exceed realistic cell speeds when  $\nabla S$  is large. In this case the microscopic time scale and macroscopic time scales are lumped together and new techniques are needed to derive macroscopic equations. Therefore the problem remains to be solved for a large signal gradient  $H \geq \mathcal{O}(1) \text{ sec}^{-1}$ , where the adaptation time  $t_a$  can vary from seconds to minutes.

**Random walk P1:** Random walk P1 is the same as random walk P except that cell velocity changes between turnings as a result of external forces, *i.e.*  $\frac{d\mathbf{v}}{dt} = \mathbf{a}$ .

**Open Problem 2:** Random walk P1 with  $\mathbf{f}$  given by (8)–(9) and  $\mathbf{a}$  as a swimming bias has been shown to predict transient spiral patterns [37] similar to what is observed. Equation (11) has been derived from random walk P1 under the shallow gradient assumption [38]. Therefore it remains to determine whether the equation (11) also has spiral solutions under certain conditions when coupled with the signal equation.

**Random walk P2:** Random walk P2 is the same as random walk P1 except that the turning rate and turning kernel also depends on the external force field, *i.e.*  $\lambda = \lambda(y, \mathbf{b})$ ,  $T = T(\mathbf{v}, \mathbf{v}', \mathbf{b})$ .

**Open Problem 3:** Chemotaxis of bacteria has the potential to facilitate waste degradation in bioremediation processes. Their bacterial movement are subject to convection by fluid as well as active swimming towards wastes. Presumably the fluid motion alters bacterial moving pattern by altering both runs and tumbles, therefore the running velocity, turning kernel and turning rate are functions of the local fluid velocity  $\mathbf{u}$  etc. The macroscopic equation that incorporates cell-fluid interaction needs to be derived and may not be a simple addition of convective flux to the chemotaxis equation.

**Open Problem 4:** A more general problem is to derive macroscopic equations that incorporate cell-cell interaction. One step in this direction is made in [20]. Another question is whether the chemotaxis equation with volume-exclusion [30] can be derived from the random walk P.

**Random walk D:** We consider a cell of type D. The position of its center evolves according to (19). Its internal state evolves according to the PDE (16)–(17). The membrane state functions evolve according to the ODE (18) where  $S$  is the external signal. The velocity evolves according to  $\mathbf{v} = \mathbf{V}(\mathbf{y})$  where  $\mathbf{V}(\mathbf{y})$  is a random variable.

**Open Problem 5:** The general question is: under what conditions can be the collective behavior of cells that undergo Random walk D be described by equation (1)? As discussed in Section 2.3, the derivation of macroscopic equations has been addressed for a simplified model of the individual behavior of cells of type D; details are given in [10]. However, even in this simplified case the macroscopic equations are not the classical chemotaxis equation (1), and whether the macroscopic equations can, under some conditions, be reduced to (1) remains an open problem. Considering a different individual-based model of the form of Random walk D, brings additional challenges to the derivation of macroscopic equations. The derivation of macroscopic equations remains open, for example, for the balanced inactivation model of Levine, *et al.*, [21] and for the intracellular model of Dd developed by Tang, Dallon and Othmer [35, 6].

## 4 Summary

We have summarized recent results and open problems in modeling the behavior of unicellular organisms, with a focus on the derivation of macroscopic equations from individual-based models. We also formulated several open problems in this area in mathematical terms. Advances in the theory of PDEs, random processes, moment closure techniques and asymptotic analysis must be made in order to resolve these problems. This makes the ‘micro-macro transition in biology’ an exciting area of current research in applied mathematics.

**Acknowledgments** This research was supported in part by NSF Grant DMS # 0817529 and NIH Grant 02911123 (HGO), by the Mathematical Biosciences Institute via a post-doctoral fellowship (CX) and by Somerville College, University of Oxford (RE). This publication is based on work supported by Award No. KUK-C1-013-04, made by King Abdullah University of Science and Technology (KAUST) (RE).

## References

- [1] H. Berg. How bacteria swim. *Scientific American*, 233:36–44, 1975.
- [2] H. Berg. *Random Walks in Biology*. Princeton University Press, 1983.
- [3] H. Berg and D. Brown. Chemotaxis in *Escherichia coli* analysed by three-dimensional tracking. *Nature*, 239:500–504, 1972.
- [4] H. Berg. Motile behavior of bacteria. *Physics Today*, 53(1):24–29, 2000.
- [5] C. Chung, S. Funamoto, and R. Firtel. Signaling pathways controlling cell polarity and chemotaxis. *Trends in Biochemical Sciences*, 26(9):557–566, 2001.
- [6] J. Dallon and H. Othmer. A continuum analysis of the chemotactic signal seen by dictyostelium discoideum. *Journal of Theoretical Biology*, 194(4):461–483, 1998.
- [7] W. DiLuzio, L. Turner, M. Mayer, P. Garstecki, D. Weibel, H. Berg, and G. Whitesides. *Escherichia coli* swim on the right-hand side. *Nature*, 435(7046):1271–4, 2005.
- [8] R. Erban and H. Othmer. From individual to collective behaviour in bacterial chemotaxis. *SIAM Journal on Applied Mathematics*, 65(2):361–391, 2004.
- [9] R. Erban and H. Othmer. From signal transduction to spatial pattern formation in *E. coli*: A paradigm for multi-scale modeling in biology. *Multiscale Modeling and Simulation*, 3(2):362–394, 2005.
- [10] R. Erban and H. Othmer. Taxis equations for amoeboid cells. *Journal of Mathematical Biology*, 54(6):847–885, 2007.
- [11] P. Fisher, R. Merkl, and G. Gerisch. Quantitative analysis of cell motility and chemotaxis in *Dictyostelium discoideum* by using an image processing system and a novel chemotaxis chamber providing stationary chemical gradients. *Journal of Cell Biology*, 108:973–984, 1989.
- [12] G. Gerisch. Chemotaxis in *Dictyostelium*. *Annual Review of Physiology*, 44:535–552, 1982.
- [13] G. Gerisch, H. Fromm, A. Huesgen, and U. Wick. Control of cell-contact sites by cyclic AMP pulses in differentiating *Dictyostelium* cells. *Nature*, 255:547–549, 1975.
- [14] S. Goldstein. On diffusion by discontinuous movements, and on the telegraph equation. *Quart. Journ. Mech. and Applied Math.*, 4(2):129–156, 1950.
- [15] T. Hillen and H. Othmer. The diffusion limit of transport equation derived from velocity-jump processes. *SIAM Journal on Applied Mathematics*, 61:751–775, 2000.
- [16] D. Horstmann. From 1970 until present: the Keller-Segel model in chemotaxis and its consequences I. *Jahresbericht der DMV*, 105(3):103–165, 2003.
- [17] C. Janetopoulos, L. Ma, P. Devreotes, and P. Iglesias. Chemoattractant-induced phosphatidylinositol 3,4,5-trisphosphate accumulation is spatially amplified and adapts, independent of the actin cytoskeleton. *Proc Natl Acad Sci U S A*, 101(24):8951–6, 2004.
- [18] M. Kac. A stochastic model related to the telegrapher’s equation. *Rocky Mountain Journal of Mathematics*, 4(3):497–509, 1974.
- [19] D. Koshland. *Bacterial Chemotaxis as a Model Behavioral System*. New York: Raven Press, 1980.
- [20] J. Lega and T. Passot. Hydrodynamics of bacterial colonies: A model. *Phys Rev E Stat Nonlin Soft Matter Phys.*, 67(3):1–18, 2003.

- [21] H. Levine, D. Kessler, and W. Rappel. Directional sensing in eukaryotic chemotaxis: A balanced inactivation model. *Proc Natl Acad Sci U S A*, 103(26):9761–6, 2006.
- [22] L. Ma, C. Janetopoulos, L. Yang, P. Devreotes, and P. Iglesias. Two complementary, local excitation, global inhibition mechanisms acting in parallel can explain the chemoattractant- induced regulation of PI(3,4,5)P3 response in dictyostelium cells. *Biophys J*, 87(6):3764–74, December 2004.
- [23] J. Mato, A. Losada, V. Nanjundiah, and T. Konijn. Signal input for a chemotactic response in the cellular slime mold *Dictyostelium discoideum*. *Proceedings of the National Academy of Sciences USA*, 72:4991–4993, 1975.
- [24] D. Morale, V. Capasso, and K. Oelschläger. An interacting particle system modelling aggregation behavior: from individuals to populations. *Journal of Mathematical Biology*, 50(1):49–66, 2005.
- [25] H. Othmer, S. Dunbar, and W. Alt. Models of dispersal in biological systems. *Journal of Mathematical Biology*, 26:263–298, 1988.
- [26] H. Othmer and T. Hillen. The diffusion limit of transport equations 2: Chemotaxis equations. *SIAM Journal on Applied Mathematics*, 62:1222–1250, 2002.
- [27] H. Othmer and P. Schaap. Oscillatory cAMP signaling in the development of *Dictyostelium discoideum*. *Comments on Theoretical Biology*, 5:175–282, 1998.
- [28] H. Othmer. On the significance of finite propagation speeds in multicomponent reacting systems. *Journal of Chemical Physics*, 64:460–470, 1976.
- [29] H. Othmer, K. Painter, D. Umlis, and C. Xue. The intersection of theory and application in biological pattern formation. *Math. Mod. Nat. Phenom.*, 2009 (to appear)
- [30] K. Painter and T. Hillen. Volume-filling and quorum-sensing in models for chemosensitive movement. *Canadian Applied Mathematics Quarterly*, 10(4):501–543, 2002.
- [31] E. Palsson and H. Othmer. A model for individual and collective cell movement in *Dictyostelium discoideum*. *Proc. Nat. Acad. Sci.*, 97(19):10448–10453, 2000.
- [32] C. Parent and P. Devreotes. A cell’s sense of direction. *Science*, 284:765–770, 1999.
- [33] P. Spiro, J. Parkinson, and H. Othmer. A model of excitation and adaptation in bacterial chemotaxis. *Proceedings of the National Academy of Sciences USA*, 94:7263–7268, 1997.
- [34] A. Stevens. The derivation of chemotaxis equations as limit dynamics of moderately interacting stochastic many-particle systems. *SIAM Journal on Applied Mathematics*, 61:183–212, 2000.
- [35] Y. Tang and H. Othmer. Excitation, oscillations, and wave propagation in *Dictyostelium discoideum*. *Philosophical Transactions of the Royal Society B: Biological Sciences*, pages 179–195, 1995.
- [36] D. Wessels, J. Murray, and D. Soll. Behavior of *Dictyostelium amoebae* is regulated primarily by the temporal dynamic of the natural cAMP wave. *Cell Motility and the Cytoskeleton*, 23(2):145–156, 1992.
- [37] C. Xue, E. Budrene-Kac, and H. Othmer. Radial and spiral stream formation in bacterium *Proteus mirabilis* colonies, 2009 (in preparation)
- [38] C. Xue and H. Othmer. Multiscale models of taxis-driven patterning in bacterial populations. *SIAM Journal on Applied Mathematics*, 2009 (to appear)
- [39] C. Xue. *Mathematical models of taxis-driven bacterial pattern formation*. PhD thesis, University of Minnesota, 2008.



## RECENT REPORTS

### 2009

01/09	A Mass and Solute Balance Model for Tear Volume and Osmolarity in The Normal And The Dry Eye	Gaffney Tiffany Yokoi Bron
02/09	Diffusion and permeation in binary solutions	Peppin
03/09	On the modelling of biological patterns with mechanochemical models: insights from analysis and computation	Moreo Gaffney Garcia-Aznar Doblare
04/09	Stability analysis of reaction-diffusion systems with time-dependent coefficients on growing domains	Madzvamuse Gaffney Maini
05/09	Onsager reciprocity in premelting solids	Peppin Spannuth Wettlaufer
06/09	Inherent noise can facilitate coherence in collective swarm motion	Yates <i>et al.</i>
07/09	Solving the Coupled System Improves Computational Efficiency of the Bidomain Equations	Southern Plank Vigmond Whiteley
08/09	Model reduction using a posteriori analysis	Whiteley
09/09	Equilibrium Order Parameters of Liquid Crystals in the Landau-De Gennes Theory	Majumdar
10/09	Landau-De Gennes theory of nematic liquid crystals: the Oseen-Frank limit and beyond	Majumdar Zarnescu
11/09	A Comparison of Numerical Methods used for Finite Element Modelling of Soft Tissue Deformation	Pathmanathan Gavaghan Whiteley
12/09	From Individual to Collective Behaviour of Unicellular Organisms: Recent Results and Open Problems	Xue Othmer Erban
13/09	Stochastic modelling of reaction-diffusion processes: algorithms for bimolecular reactions	Erban Chapman
14/09	Chaste: a test-driven approach to software development for physiological modelling	Pitt-Francis <i>et al.</i>

15/09	Block triangular preconditioners for PDE constrained optimization	Rees Stoll
16/09	From microscopic to macroscopic descriptions of cell migration on growing domains	Baker Yates Erban

**Copies of these, and any other OCCAM reports can be obtained from:**

**Oxford Centre for Collaborative Applied Mathematics  
Mathematical Institute  
24 - 29 St Giles'  
Oxford  
OX1 3LB  
England**

**[www.maths.ox.ac.uk/occam](http://www.maths.ox.ac.uk/occam)**